

# Positron annihilation studies of fluorine-vacancy complexes in Si and SiGe

C. J. Edwardson,<sup>1,a)</sup> P. G. Coleman,<sup>1</sup> H. A. W. El Mubarek,<sup>2</sup> and A. S. Gandy<sup>2</sup><sup>1</sup>Department of Physics, University of Bath, Bath BA2 7AY, United Kingdom<sup>2</sup>School of Electrical and Electronic Engineering, University of Manchester, Manchester, M13 9PL, United Kingdom

(Received 16 December 2011; accepted 28 February 2012; published online 4 April 2012)

The formation of fluorine-vacancy (FV) complexes in strained Si-SiGe-Si multilayer structures and relaxed SiGe layers of varying Ge content has been investigated using variable-energy positron annihilation spectroscopy, including Doppler-broadened spectra ratio curves. It has been found that in all sample types there are two distinct regions defined only by the damage created by the implanted F ions. The first, shallower region (from the surface to a depth of  $\sim 200$  nm) was found to contain a mixture of undecorated vacancies and FV complexes; there is no correlation between the vacancy or F concentration in this region and the Ge content. The multi-layer samples may also have O contamination that is not present in the relaxed samples. The second region (at depths  $\sim 200$ – $440$  nm) contains primarily FV complexes in all samples. In the multi-layer samples secondary ion mass spectrometry (SIMS) results show peaks of F accumulating in, or at the interfaces of, each SiGe multi-layer; the FV complexes, however, are distributed over depths similar to those in the relaxed samples, with some localization at the SiGe layer located within the second region. The positron response is primarily to FV complexes formed by the F implant in all samples. The F: FV ratios are approximately 3–7: 1 in the relaxed samples. Positrons appear to be relatively insensitive to the largest of the F SIMS peaks which lies beyond the second region. This is probably because the F has filled all the open volume at the SiGe layer, leaving no positron trapping sites. © 2012 American Institute of Physics. [<http://dx.doi.org/10.1063/1.3699314>]

## I. INTRODUCTION

The effect of fluorine on the behavior of vacancies (V) and interstitials (I) in Si has been of great interest to researchers in the past<sup>1</sup> due its effectiveness in reducing transient-enhanced diffusion of dopants such as boron. For example, limiting B diffusion would allow the formation of ultra-shallow junctions. This can be achieved via the formation of fluorine-vacancy (FV) and fluorine-interstitial (FI) complexes.<sup>2</sup>

Recently, strained SiGe layers have been a subject of interest as they have been shown to produce high electron mobility transistors, much higher than in relaxed materials.<sup>3</sup> Kögler *et al.* reported on the behavior of V and I in SiGe, showing that ion-induced damage in SiGe is higher than in Si and increases with increasing Ge content.<sup>4</sup> It was found that in SiGe the Ge content impedes vacancy-interstitial defect recombination. However, not much is known about the effect of F on the behavior of V and I in SiGe. Positron annihilation spectroscopy (PAS) has been used to investigate vacancy-dopants complexes in SiGe,<sup>5</sup> which concluded that the presence of Ge around a vacancy is not enough to make divacancy defects stable at room temperature. In our previous report,<sup>6</sup> the effect of F in a layered HBT-type structure of Si-SiGe-Si was investigated using variable-energy PAS (VEPAS) with the main result showing that  $F_{4n}V_n$  complexes are associated with the SiGe layer and that they preferentially accumulate at the Si/SiGe interfaces. Here this work is

extended and VEPAS is used to investigate the effect of F in multiple strained Si-SiGe layers and relaxed SiGe.

## II. EXPERIMENT AND ANALYSIS

Relaxed SiGe layers,  $1\ \mu\text{m}$  thick, having Ge fractions of 10%, 20% or 30% were deposited by reduced pressure chemical vapor deposition onto a graded SiGe layer with linearly decreasing Ge% (10% per  $\mu\text{m}$ ) on a p-type Si (100) substrate. Compressively strained Si-SiGe-Si multi-layers with Ge fractions of 10% (50 nm), 20% (30 nm), and 30% (10 nm) with  $\sim 100$  nm of Si in between each layer. The different layer widths shown in brackets were used to retain strain in the SiGe. F ions were implanted into the samples at room temperature with an energy of 185 keV at a fluence of  $2.3 \times 10^{15}\ \text{cm}^{-2}$ . The samples were rapid thermal annealed in a N atmosphere for 20 s at  $800^\circ\text{C}$ .

In VEPAS positrons are implanted into a sample with energies  $E$  between 0.25 and 30 keV. These energies dictate the positron implantation profile enabling depth profiling from the surface to a depth dependent principally on the material's density. Implanted positrons rapidly thermalize and diffuse to either annihilate free electrons or become trapped in vacancy-type defects and interfaces finally annihilating with two approximately anti-collinear 511 keV  $\gamma$ -rays. Momentum of the electrons at the annihilation site causes the 511 keV line to broaden; this broadening is measured using a high-purity Ge detector and characterized using the  $S$  parameter<sup>7</sup> defined as the fraction of the annihilation line in the central region. The  $S$  parameter has a characteristic value for each type of annihilation site including vacancy-type

<sup>a)</sup>Author to whom correspondence should be addressed. Electronic mail: c.j.edwardson@bath.ac.uk.

defects. Analysis of  $S$  as a function on energy,  $S(E)$ , can provide depth-dependent information. VEPFIT (Ref. 8) is a fitting program which takes the raw  $S(E)$  data and solves the positron diffusion equation to calculate the characteristic  $S$  parameter for each region within the sample.

The ratio curve technique measures – also with a single Ge detector – the annihilation line, or spectrum, peaked at 511 keV with high precision to extract further information from the higher momentum components contained in its wings. Core electrons have a characteristic momentum associated with their atom enabling chemical analysis of the species that surround the annihilation site.<sup>9</sup> Positrons are implanted at a single energy where the response is the greatest for the region of interest. The spectrum, collected typically for  $\sim 48$  h, is normalized to an area of  $1.5 \times 10^8$  counts between 491 and 531 keV and divided by the reference spectrum of undefected Si to reveal any differences in the high momentum content between 511 and 531 keV. This difference is the response to the chemical composition of the environment surrounding a positron-trapping defect, such as a vacancy. The response can be due to the presence of one type of atom or defect type but in more complex systems it can be formed from combinations of all the pure states that lie within the region of the implantation profile, e.g., F, V<sub>2</sub> in Si, Ge, and O. By fitting combinations of these pure states, each with its own unique signature, a more detailed picture of the vacancy complexes in the region of interest can be found.

Initial F implantation and Si and Ge defect profiles were simulated with the program SRIM (Stopping and Range of Ions in Matter).<sup>10</sup> A concentration depth profile of F after annealing was measured using secondary ion mass spectrometry (SIMS).

### III. RESULTS AND DISCUSSION

#### A. Positron affinity for Si and Ge

To investigate the chemical composition of the defect environment created by ion implantation and annealing the relative positron affinity for Ge and Si first needed to be known. The unimplanted samples were etched in hydrofluoric acid to remove any surface oxide response and spectra were taken at a single energy where the mean implantation depth of the positrons was within the first micron. The spectra were normalized to Si. It was found that after removing a percentage of a Ge/Si peak equal to the Ge content of each sample the ratios are  $\sim 1$  overall energies, meaning that only a response to Si remained, as seen in Fig. 1. This result indicates that there is essentially the same relative positron affinity for both Si and Ge and that this technique can be used to obtain quantitative information, as discussed in Ref. 11.

#### B. As-implanted samples

After implantation the  $S(E)$  results (Fig. 2, only 10% and 30%Ge samples shown for clarity) for the relaxed SiGe samples show that as the percentage of Ge increases the average  $S$  parameter in the saturated region (3–10 keV)

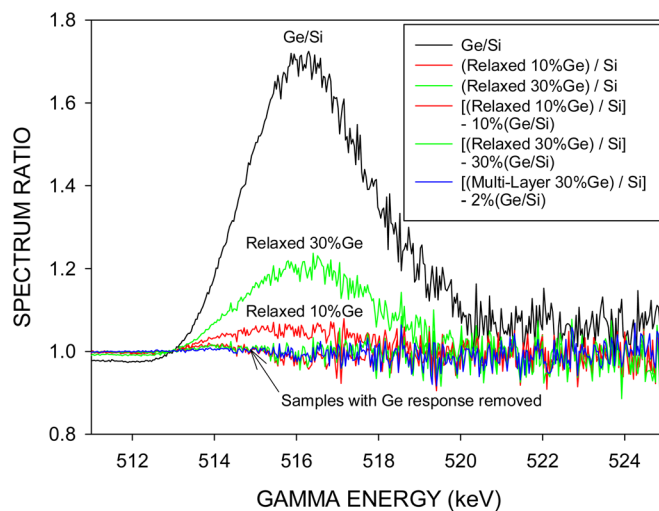


FIG. 1. Ratios of the unimplanted samples of relaxed 10% and 30%Ge and multi-layer 30%Ge, before and after removal of Ge ratio response. (Multi-layer 30%Ge is not shown before Ge removal for clarity.) The ratio for Ge/Si is shown for reference. All spectra are divided by a Si spectrum.

decreases slightly. This was as expected because Ge has a lower  $S$  parameter than Si. However, the multi-layer samples (again only 10% and 30%Ge samples shown for clarity) show that as the percentage of Ge increases, the average  $S$  parameter in the saturated region (3–10 keV) increases slightly. It is believed this is due to the width of the Ge layers, where the 30%Ge sample had the narrowest SiGe layers and the widest Si layers and therefore would have the lowest response to Ge.

All the fits to the data for the as-implanted samples, obtained using VEPFIT, were similar, with only slight variations in the V-rich defected region  $S$  parameter, as suggested by the raw data in Fig. 2. The saturated region has a normalized  $S$  parameter below that for both di-vacancies in Si ( $S \sim 1.04$ ) and amorphous Si (A-Si) ( $S \sim 1.03$ ). An  $S$  parameter of  $\sim 1.04$  has been shown to be the characteristic  $S$  of an isolated di-vacancy in Ge (normalized to bulk Ge), which is reduced to  $\sim 1.02$  if normalized to bulk Si (previous measurements of the ratio of bulk Ge to bulk Si

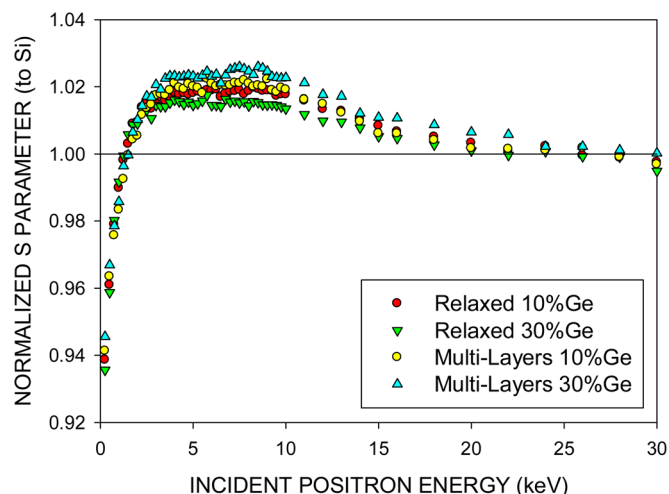


FIG. 2. Normalized  $S(E)$  plot for as-implanted relaxed and multi-layer samples of 10% and 30%Ge.

parameters have been  $\sim 0.98$ ).<sup>12</sup> It is extremely unlikely that there is just this single type of defect when the largest proportion of the sample is Si; therefore, a mixture of defect types are instead contributing to the  $S$  parameter.

To determine what these defect types could be, combinations of likely elements and states were compared to the measured spectral ratio data in order to gain a best fit. In this case amorphous Ge (A-Ge), Ge, Si,  $V_2$  in Si and A-Si were considered. Examples can be seen in Fig. 3. Data for the relaxed 10%Ge, relaxed 30%Ge, and 30%Ge multi-layer samples at 6 keV had best fits of [15%Ge + 85%A-Si], [30%Ge + 70%A-Si], and [5%Ge + 95%A-Si], respectively. The uncertainties in these percentages can be up to  $\pm 5\%$ , as fits are assessed by eye. The use of spectra ratio data for A-Si does not necessarily imply that the Si was amorphized by the implant, but rather that the Si structure was disordered – possibly containing  $V_n$  for which spectral data was not available. The positron sensitivity to Ge seems to remain unchanged and still looks like a Ge response rather than A-Ge. These fits imply an even distribution of vacancy defects within the material and are consistent with the  $S(E)$  data, which can be reproduced using the fitted percentages and the characteristic  $S$  values for Ge and A-Si. The fits to the spectra for multi-layer samples have much lower Ge percentages because of the smaller overlap in the positron implantation profile with the thin SiGe layers.

### C. Annealed samples

After annealing the remaining damage can be seen as peaks (vacancy-rich defects) and dips (FV complexes),<sup>2</sup> at 3 and 6 keV, respectively, in the example  $S(E)$  data in Fig. 4. This pattern can be seen in all samples, although there are slightly different apparent depths corresponding to the peaks and dips due to differences in sample density affecting the positron implantation profile. There appears to be little correlation between the peak/dip  $S$  parameters and the Ge content in all samples, so ratio curves were taken at each peak and

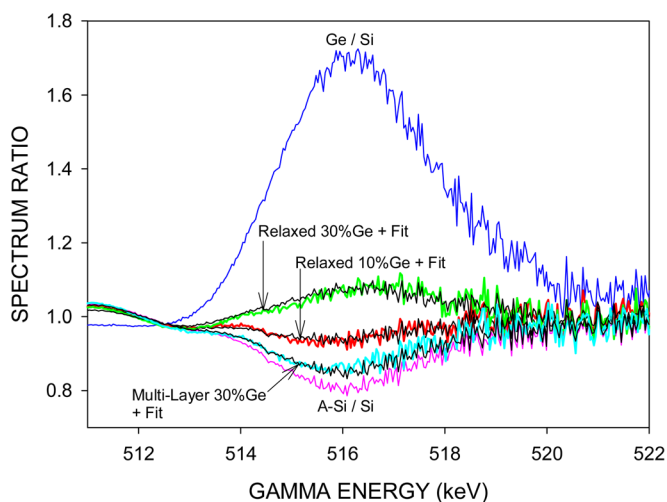


FIG. 3. Ratios of the as-implanted samples of relaxed 10% and 30%Ge and multi-layer 30%Ge at 6 keV. Best fits are shown on top of the data. Ratios of Ge/Si and A-Si are shown for reference. All spectra are divided by a Si spectrum.

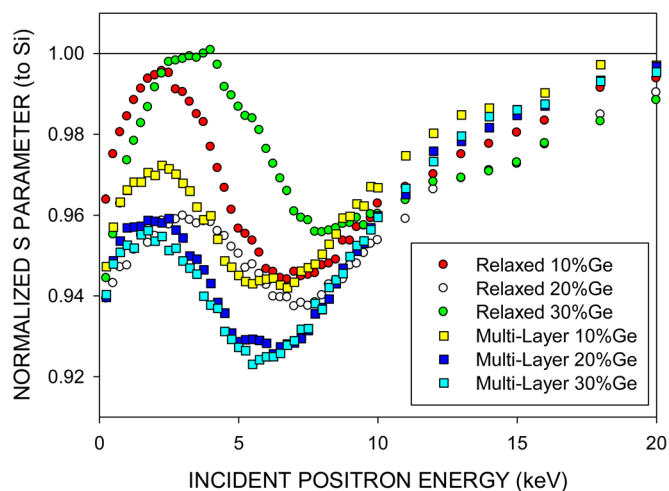


FIG. 4. Normalized  $S(E)$  plot for annealed relaxed and multi-layer samples of 10%–30%Ge.

dip to try to determine the nature of the defects and the reasons for the differences between samples. It is important to recognize that since ratio curves are taken at one implantation energy their response will be due to annihilations over the whole of the implantation profile, not just at the depth of interest, so the following fits can only give an idea of the defects' chemical composition.

Reference spectra for Ge, F,  $V_2$  in Si, Si and implanted  $SiO_2$  (for an O response) were used to fit the lower energy peaks seen in Fig. 5. The relaxed samples had good fits with a large % of F and  $V_2$  with the remaining contributions being from free positron annihilation in Ge and Si in their original ratios. For example, the 10%Ge sample could be fit well with [5%Ge + 45%Si + 23%F + 27% $V_2$ ] and the 30%Ge sample with [20%Ge + 40%Si + 10%F + 30% $V_2$ ]. The heights of the peaks in  $S(E)$  seem to depend on the F content, i.e., there are FV complexes as well as divacancy defects in this region. The multi-layer samples, however, could not be fit well with the expected F, Si, and  $V_2$  curves; instead fits were found

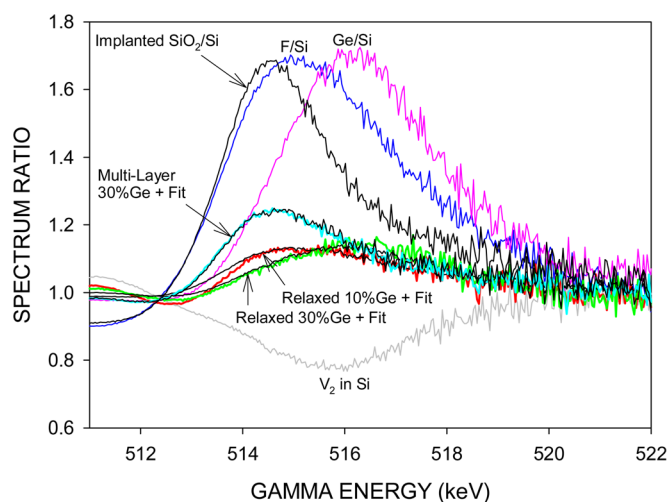


FIG. 5. Ratios of the annealed samples of relaxed 10% and 30%Ge and multi-layer 30%Ge at  $\sim 2$  keV. Best fits are shown on top of data. Ratios of implanted  $SiO_2$ /Si, F/Si, Ge/Si, and  $V_2$  in Si/Si are shown for reference. All spectra are divided by a Si spectrum.



containing F, Si, and O. For example the spectrum for the 30%Ge sample was fit well with [10%F + 64%Si + 26%O] (there is no Ge response since the first SiGe layer is deeper than the low-energy peak). The multi-layer samples appear to have an O response in this damaged region whereas the relaxed samples did not. The SIMS analysis did not include oxygen.

The spectra ratios for the higher-energy dips seen in Fig. 6 were fit with Ge, F, and Si. This region is thought to be mainly populated by FV complexes. These spectra were successfully fit in both the relaxed and the multi-layer samples. Relaxed 10%Ge, for example, was fit by [10%Ge + 65%F + 25%Si] and 30%Ge by [30%Ge + 42%F + 28%Si]. These fits do not follow the same pattern as those for the lower-energy vacancy-rich peaks in that the Ge/Si ratio has changed. The fitted Ge% matches that of the as-grown samples, suggesting that, in this case, the F could be preferentially combining with vacancies in Si, since the positron response to Ge remains the same while some of the response to Si is replaced by F. The multi-layer samples were fit in the same way - e.g., 30%Ge had [10%Ge + 84%F + 6%Si]. All three multi-layer samples had this 10%Ge response with only the F content varying and changing the  $S$  parameter.

#### D. Comparison with SRIM and SIMS results

The positron data can be further interpreted using information gained from SIMS. Figures 7(a) and 7(b) show examples of VEPAS (with VEPFIT fits), SRIM and SIMS results plotted together. The VEPAS depths are mean positron implantation depths, and at each depth the FWHM of the positron depth profile is approximately equal to the mean depth. Therefore, the response becomes progressively smeared as the depth increases. However, the fitting code VEPFIT takes this into account.

The following summarizes the main elements of Figs. 7(a) and 7(b), which are common to both relaxed and multi-layer samples.

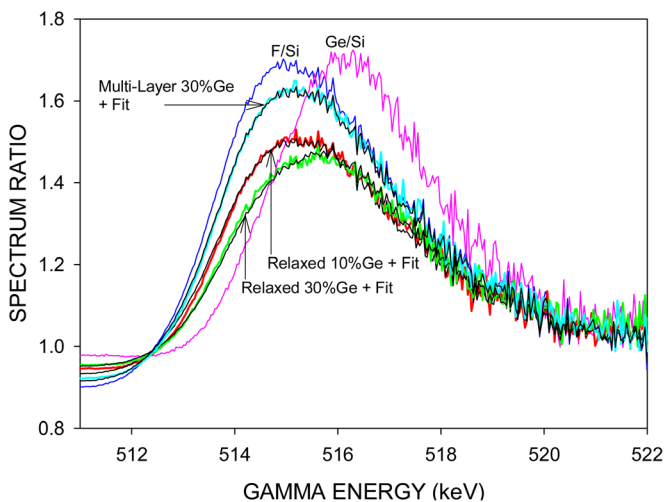


FIG. 6. Ratios of the annealed samples of relaxed 10 and 30%Ge and multi-layer 30%Ge at  $\sim 7$  keV. Ratios of implanted F/Si and Ge/Si are shown for reference. All spectra are divided by a Si spectrum.

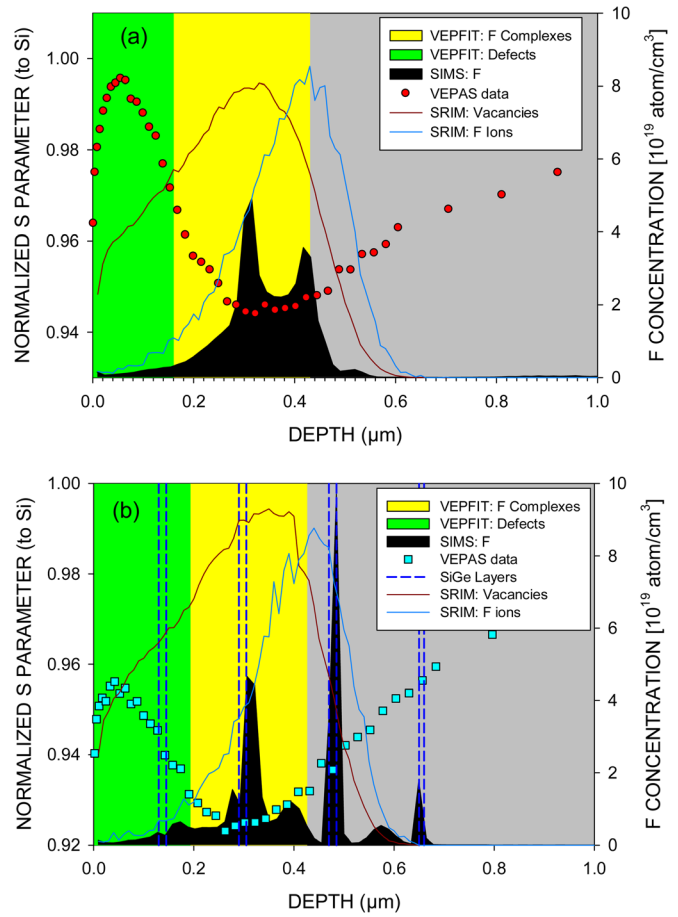


FIG. 7. All depth dependent data are shown for the annealed relaxed sample of 10%Ge (a) and the multi-layer sample of 30%Ge (b). The left-hand axis corresponds to the normalized  $S(E)$  plot and the right-hand axis corresponds to the SIMS F concentration data. Other plots include the two VEPFIT regions of F complexes and vacancy-rich defects and the initial Si and Ge vacancy and F ion profiles.

VEPAS data (left-hand axis) are fit by VEPFIT into three distinct regions: the topmost region having a short positron diffusion length but high  $S$  parameter, suggesting a vacancy-rich region, most probably a mixture of undecorated vacancies and FV complexes. The second region has a short positron diffusion length and low  $S$ , suggesting a FV-rich region. The third region is the Si substrate.

SRIM simulations show the initial F implantation profile and the resulting Si and Ge vacancy profiles before annealing. SIMS intensity plots (right-hand axes) are shown for F after annealing. The double F-peak feature seen in the relaxed samples had similar profiles, an example of one can be seen in Fig. 7(a). Originally a 9-region model was used in VEPFIT for the strained multi-layer samples, on the assumption that all the FV complexes were confined to the SiGe layers (as suggested by the SIMS F peaks). The model assumed zero diffusion in the SiGe layers, i.e., saturated positron trapping because of the high concentration of FV in these layers. However, the fitted  $S$  parameter for these layers was considerably higher (i.e.,  $>0.91$ ) than that expected for 100% trapping in F complexes.<sup>13</sup> Also, the third SiGe layer from the surface always had the greatest SIMS F concentration but there was no response to it in any of the  $S(E)$  plots,

as is demonstrated by the example data in Fig. 7(b). An alternative VEPFIT model was therefore required in which the vacancies created by the implanted F form complexes with F in a similar region in each sample. The dip in the  $S$  parameter caused by the F is always seen in the middle of this region; this depth is that of the peak of Ge and Si vacancies caused by the initial F implantation damage as calculated by SRIM. The F SIMS for each of the multi-layer samples had very similar profiles, an example of one can be seen in Fig. 7(b). In the first SiGe layer at  $\sim 150$  nm there was almost no pile-up of F, the average concentration was similar to that in the surrounding Si. The second SiGe layer at  $\sim 300$  nm always lay close to the center of the dip in the  $S(E)$  plots. The concentration of F in this layer was significantly higher than in the first and similar to that seen in the relaxed samples at the same depth (see Fig. 7(a)). Extra disorder in the SiGe layer may be trapping and localizing F but it is the initial implantation damage causing the formation of FV complexes. The third SiGe layer at  $\sim 500$  nm contained the greatest concentration of F, this layer becomes saturated with F atoms leaving few open volume defects effectively becoming invisible to VEPAS thereby showing a similar depth response to that in the relaxed SiGe samples.

A 3-region VEPFIT model was thus used for both the strained multi-layer and relaxed samples, fitting a region of vacancy defects  $\sim 200$  nm wide followed by a  $\sim 240$  nm wide FV complex region and bulk Si for all samples.

Using SIMS and VEPFIT data the 3-region model was further analyzed to obtain average concentrations of  $V_2$  ( $C_{V2}$ ) and FV ( $C_{FV}$ ) in the top region, and the ratio of F to V in the second region. To analyze the top region ( $\sim 0$ – $200$  nm) the average concentration of F ( $C_F$ ) was found from SIMS data in the same region. The average  $C_{FV}$  and  $C_{V2}$  were found using the ratio curve fits, from the fraction trapped in F and  $V_2$ , respectively. These can be used for the top region as the implantation profile lies completely within it. Both concentrations were derived using

$$C = 5 \times 10^{22} [f \lambda_B / \nu (1 - f)] \text{ cm}^{-3} \quad (1)$$

since there are multiple types of trapping defect, where  $f$  is the trapped fraction found from the ratio curves,  $\lambda_B$  is the positron annihilation rate in perfect Si ( $4.54 \times 10^9 \text{ s}^{-1}$ ),<sup>14</sup> and  $\nu$  is the specific trapping rate for positrons in a trapping defect which was assumed to be  $10^{15} \text{ s}^{-1}$  for the FV complexes and  $7 \times 10^{14} \text{ s}^{-1}$  for divacancies. If the FV complexes were  $F_{4n}V_n$  (where  $n$  is most likely to be 1 or 2) then for example in the relaxed 10%Ge sample 15%–30% of the total F, according to SIMS, is in complexes, with the rest left as isolated F, agglomerates or precipitates, as seen before.<sup>6</sup> A summary of results for the relaxed samples' top region can be seen in Table I.

There appears to be little correlation between the Ge content and vacancy concentration. The low percentage of F in complexes in the relaxed 30%Ge sample is due to the low  $C_{FV}$  in the sample derived from the high  $S$  parameter.

The top region for the multi-layer samples was analyzed in the same way but only  $C_{FV}$  was deduced as any  $V_2$  response was masked by the O response. The concentration

TABLE I. Concentrations of F, FV, and  $V_2$  in the top region of relaxed samples.

Sample (Relaxed)	$C_F$ from SIMS ( $10^{18} \text{ cm}^{-3}$ )	$C_{FV}$ ( $10^{16} \text{ cm}^{-3}$ )	$C_{V2}$ ( $10^{17} \text{ cm}^{-3}$ )	%F in $F_{4n}V_n$ $n = 1/2$
10%Ge	1.7	7	1	15/30%
20%Ge	5.3	16	0.8	12/24%
30%Ge	6.3	2.5	1.4	2/4%

of oxygen complexes ( $C_O$ ) was calculated assuming the trapping rate was the same as that used for FV complexes. The results are shown in Table II.

F is possibly being displaced by the presence of more oxygen in the 20% and 30% multi-layer samples causing fewer F to complex with vacancies.

The ratio curve fits cannot be used to find  $C_{FV}$  in the second region since the fraction trapped is in the region of the implantation profile, not just the second region. They can however be used to find  $S$  for FV complexes ( $S_D$ ). Knowing the  $S$  parameter for Ge (0.98) and Si (1) and finding the total  $S$  from the  $S(E)$  data at the energy measured the  $S$  parameter for the FV complexes in all samples was found to be  $0.91 \pm 0.01$ .

Analyzing the second region in the relaxed samples again required the  $C_F$  for the region ( $\sim 200$ – $440$  nm) to be found from SIMS. The  $C_F$  in the multi-layer samples also includes the whole region, including the peak, as the two contributions cannot be distinguished in the present samples. To do so would require samples with SiGe layers outside the region of ion damage. The  $C_{FV}$  was derived using the  $S$  parameter fitted for the region, rather than using the ratio fits as the implantation profile now extends beyond the limits for the region and there is only one type of trapping defect thought to be in this region. Using

$$C_D = 5 \times 10^{22} [\lambda_B (S - S_B) / \nu (S_D - S)] \text{ cm}^{-3}, \quad (2)$$

where  $\nu$  is the specific trapping rate for positrons in a FV defect which again was assumed to be  $10^{15} \text{ s}^{-1}$ ,  $S_B$  is the bulk  $S$  parameter ( $\sim 1$ ) and  $S_D$  is assumed to be 0.91. To find the  $S$  parameter for the second region VEPFIT was used to fit the  $S$  with the constraint that it was consistent with the positron diffusion length  $L$  fitted for the same region. A summary of results for the second region of each sample is given in Table III.

The ratios of F per FV complex for the relaxed samples and the 10%Ge multi-layer sample are consistent with  $F_{4n}V_n$  (where  $n = 1$  and/or 2). The 20% and 30% multi-layer

TABLE II. Concentrations of F, FV, and O in the top region of multi-layer samples.

Sample (Multi-Layer)	$C_F$ from SIMS ( $10^{18} \text{ cm}^{-3}$ )	$C_{FV}$ ( $10^{16} \text{ cm}^{-3}$ )	$C_O$ ( $10^{16} \text{ cm}^{-3}$ )	%F in $F_{4n}V_n$ $n = 1/2$
10%Ge	2.1	7	4	13/26%
20%Ge	2.4	2.5	8	4/8%
30%Ge	2.7	2.5	8	4/8%

TABLE III. Concentrations of F and FV in the second region of all samples.

Sample	$C_F$ from SIMS ( $10^{19} \text{ cm}^{-3}$ )	$C_{FV}$ ( $10^{18} \text{ cm}^{-3}$ )	F: FV
10%Ge (Relaxed)	1.8	7	3: 1
20%Ge (Relaxed)	3.0	5	6: 1
30%Ge (Relaxed)	1.3	2	7: 1
10%Ge (Multi-Layer)	1.0	6.5	2: 1
20%Ge (Multi-Layer)	1.1	41	1: 4
30%Ge (Multi-Layer)	1.3	41	1: 3

samples, however, have unrealistic ratios. It is believed this is caused by the increased uncertainty in the fitted  $S_D$  with high concentrations of  $C_{FV} - L$  can vary significantly with small changes in  $S$  when close to saturation.

#### IV. CONCLUSION

The positron results presented here suggest that for all samples, both relaxed and multi-layer, there exist two regions defined by the depth profile of the implanted F ions. The first, shallower region (from the surface to  $\sim 200 \text{ nm}$ ) contains a mixture of undecorated vacancies (possibly  $V_2$ ) and FV complexes; there is no correlation between the vacancy or F concentrations in this region and the %Ge. The multi-layer samples may have an O contamination that is not present in the relaxed samples. The second region (from  $\sim 200$  to  $440 \text{ nm}$ ) contains primarily FV complexes. Interestingly, the positrons appear to be relatively insensitive to the highest concentrations of F in the third SiGe layers, i.e., the FV complexes do not reside primarily in this layer, but instead are distributed over depths similar to those in the relaxed samples as it is the initial damage caused by the F implant that facilitates the formation of FV rather than the SiGe layers as previously thought. The F: FV ratios are approximately 3–7: 1 in the relaxed samples, and 2: 1 in the 10%Ge multi-layer sample, consistent with  $F_{4n}V_n$  (where

$n = 1$  and/or 2) as has been seen before. However, ratios cannot be calculated with precision for the 20% and 30%Ge multi-layer samples due to large uncertainties in  $C_{FV}$  close to saturation.

#### ACKNOWLEDGMENTS

Dr. H. A. W. El Mubarek would like to acknowledge The Royal Academy of Engineering and EPSRC for funding her Research Fellowship. Dr. El Mubarek also acknowledges EPSRC for funding this research through an EPSRC First Grant No. EP/G0162332/1. She would also like to acknowledge Dr. Andy Smith at the University of Surrey Ion Beam Centre for the Ion Implantation and Rapid Thermal Annealing Processing of the samples studied in this work.

- <sup>1</sup>H. A. W. El Mubarek and P. Ashburn, *Appl. Phys. Lett.* **83**, 4134 (2003).
- <sup>2</sup>X. D. Pi, C. P. Burrows, and P. G. Coleman, *Phys. Rev. Lett.* **90**, 155901 (2003).
- <sup>3</sup>F. Schäffler, *Semicond. Sci. Technol.* **12**, 1515 (1997).
- <sup>4</sup>R. Kogler, A. Mucklich, W. Skorupa, A. Peeva, A. Y. Kuznetsov, J. S. Christensen, and B. G. Svensson, *J. Appl. Phys.* **101**, 033508 (2007).
- <sup>5</sup>J. Slotte, *Nucl. Instrum. Methods Phys. Res. B* **253**, 130 (2006).
- <sup>6</sup>D. A. Abdulmalik, P. G. Coleman, H. A. W. El Mubarek, and P. Ashburn, *J. Appl. Phys.* **102**, 013530 (2007).
- <sup>7</sup>A. van Veen, H. Schut, and P. E. Mijnders, in *Positron Beams and Their Applications*, edited by P. G. Coleman (World Scientific, Singapore, 2000), p. 191.
- <sup>8</sup>A. van Veen, H. Schut, J. de Vries, R.A. Hakvoort, and M.R. Ijpma, *AIP Conf. Proc.* **218**, 171 (1990).
- <sup>9</sup>K. G. Lynn and A. N. Goland, *Solid State Commun.* **18**, 1549 (1976).
- <sup>10</sup>J. F. Ziegler, J. P. Biersack, and U. Littmark, *The Stopping and Range of Ions in Matter* (Pergamon, New York, 1985).
- <sup>11</sup>P. J. Simpson, Z. Jenei, P. Asoka-Kumar, R. R. Robison, and M. E. Law, *Appl. Phys. Lett.* **85**, 1538 (2004).
- <sup>12</sup>J. Slotte, M. Rummukainen, F. Tuomisto, V. P. Markevich, A. R. Peaker, C. Jeaynes, and R. M. Gwilliam, *Phys. Rev. B* **78**, 085202 (2008).
- <sup>13</sup>D. A. Abdulmalik, P. G. Coleman, N. E. B. Cowern, A. J. Smith, B. J. Sealy, W. Lerch, S. Paul, and F. Cristiano, *Appl. Phys. Lett.* **89**, 052114 (2006).
- <sup>14</sup>S. Dannefaer, *J. Phys. C* **15**, 599 (1982).